Structural Monitoring and Maintenance, *Vol. 11, No. 2 (2024) 127-148*
https://doi.org/10.12989/smm.2024.11.2.127

Development of tension estimation method without damper modeling error for cable with damper

Aiko Furukawa*[1], Yuma Sugimachi[1] and Tomohiro Takeichi[2]

[1]Department of Urban Management, Graduate School of Engineering, Kyoto University, Kyotodaigaku-katsura, Nishikyo-ku, Kyoto-shi, Kyoto 615-8540, Japan
[2]Kobelco Wire Company, Ltd., 10-1, Nakahama-cho. Amagasaki-shi, Hyogo 660-0091, Japan

(*Received May 12, 2024, Revised June 13, 2024, Accepted June 15, 2024*)

Abstract. Estimating cable tension is important in the maintenance of cable structures, such as cable-stayed bridges. In practice, the higher-order vibration method based on natural frequencies is used. In recent years, dampers have been installed onto cables to suppress aerodynamic vibration. Because the higher-order vibration method is suitable to cables without a damper, the damper must be removed before using this method. Because damper removal is time-consuming and labor-intensive, a previous study proposed a tension estimation method for a cable with a damper based on the natural frequencies, which does not require the damper's removal. However, the previous method relies on the modeling accuracy of the damper's complex stiffness. The damper design formula, while intended for design purposes, does not consistently reflect the damper's actual complex stiffness. Therefore, the estimation accuracy deteriorates when the damper's actual complex stiffness deviates from the damper design formula. With this background, this paper introduces a novel tension estimation method based on mode shapes, which circumvents damper modeling errors since mode shapes are independent of the damper's complex stiffness. In the numerical verification using 90 models, the proposed method estimated tension accurately with an estimation error within 0.59%. In the experimental verification, the proposed method estimated tension accurately with an estimation error within 4.17% except for one case, while the previous method had an estimation error of 44% when the damper design formula was used. The proposed method was found to be superior to the previous method in terms of accuracy and practicality by numerical simulation and experiment.

Keywords: cable tension estimation; damper; damper modeling; mode shape

1. Introduction

Japan's cable structure maintenance protocols mandate the assessment of cable tension every 5 years. This evaluation predominantly relies on determining the cable tension based on the natural frequencies of cables, using either the vibration method (Shinke *et al.* 1980, Zui *et al.* 1996) or higher-order vibration method (Yamagiwa *et al.* 2000).

The vibration method relies on string theory. However, unlike strings, bridge cables possess bending stiffness. Therefore, a correlation factor is introduced to account for the cable's bending stiffness. Nevertheless, determining the bending stiffness beforehand poses a significant challenge,

*Corresponding author, Associate Professor, E-mail: furukawa.aiko.3w@kyoto-u.ac.jp

http://www.techno-press.org/?journal=smm&subpage=7 ISSN: 2288-6605 (Print), 2288-6613 (Online)

particularly because bridge cables typically comprise stranded wires, for which a theoretical bending stiffness calculation formula is lacking.

The higher-order vibration method relies on tensioned Euler–Bernoulli beam theory, and expresses the natural frequency of the cable as a function of tension and bending stiffness, enabling the simultaneous estimation of tension and bending stiffness from the natural frequencies. Therefore, this method has become widespread in engineering practice.

Various studies have investigated methodologies for estimating cable tension, including diverse scenarios such as intricate boundary conditions (Chen *et al.* 2016, 2018, Yan *et al.*2019) and uncertain boundary conditions in short cables (Li *et al.* 2021), inclined cables (Ma 2017, Kim and Park 2007), cables with flexible supports (Foti *et al.*2020), and cables connected by an intersection clamp (Furukawa *et al.* 2022a, 2022b, 2022c). Additionally, research has addressed environmental temperature variations (Ma *et al.* 2021), and methods employing genetic algorithms and particle swarm optimization (Zarbaf *et al.* 2017), neural networks (Zarbaf *et al.* 2018), deep learning (Jeong *et al.* 2020), and noncontact vision-based approaches (Liu *et al.* 2023).

Recently, attention has been increasingly given to the aerodynamic vibration of cables, and dampers are being implemented to mitigate the vibration. However, damper installation alters the cable's natural frequencies, and temporary removal is needed for tension estimation when using vibration methods. Given the time-consuming and labor-intensive nature of detaching and reattaching the dampers, there is a need for a tension estimation method that does not require removing dampers from the cable.

While previous studies have primarily focused on optimizing the damper design to suppress cable vibration (Izzi *et al.* 2016, Javanbakht *et al.* 2019, Krenk 2000, Lazar *et al.* 2016, Pacheco *et al.* 1993, Shi and Zhu 2018, Tabatabai and Mehrabi 2000), scant attention has been given to tension estimation methods for cables with dampers. Some studies (Shan *et al.* 2019, Yan *et al.* 2020), have proposed tension estimation approaches for cables with additional dampers, assuming that the damper parameters are known, which might not always be the case. Hou *et al.* (2020) introduced a tension estimation approach employing the substructure isolation method, which isolates the cable section without a damper using virtual supports. However, the installation of virtual supports may be time-consuming and labor-intensive.

Methods for cables with a single damper have been developed based on the tensioned Euler–Bernoulli beam theory for cable modeling and complex stiffness for damper modeling, providing theoretical equations for cable tension estimation from the natural frequencies (Furukawa *et al.* 2021a, 2022d, 2022e) or a combination of natural frequencies and mode shapes (Furukawa *et al.*2022f). Furthermore, a method for estimating tension from the natural frequencies for cables equipped with two dampers has been proposed (Furukawa *et al.* 2023).

In the experimental verification of the authors' previously proposed methods (Furukawa *et al.* 2022f, 2023), high-damping rubber dampers were attached to the cable, and the damper's complex stiffness was modeled using the design formula of the high-damping rubber damper. However, the authors identified a problem: the damper's actual behavior does not agree with the behavior predicted by the damper design formula, which compromises the tension estimation accuracy in the previous study (Furukawa *et al.* 2023).

It is commonly acknowledged that the damper's behavior changes depending on the frequency and amplitude (Weber and Distl 2015). However, the design formula for high-damping rubber dampers does not account for frequency dependence and amplitude dependence. In the authors' previous study (Furukawa *et al.* 2023), the damper design formula was refined such that the theoretical natural frequencies match the measured natural frequencies by introducing the frequency dependent term into the damper's complex stiffness. By combining the method previously proposed by the authors and the refined damper formula, the tension estimation accuracy was improved. However, the method still does not consider the damper's amplitude dependence.

Building upon this, the primary objective of this study is to develop a tension estimation method independent of damper modeling errors, which can be achieved by omitting the mechanical model of the damper. In previous methods, the formulation was carried out using force balance equations at the damper installation position, where the mechanical model of the damper was employed. In the proposed method, by introducing new constraint equations related to mode shapes, the force balance equation becomes unnecessary, thus achieving tension estimation independent of the mechanical model of the damper. This paper presents the formulation of the proposed method and its validation through numerical investigation and experiments. In the experimental validation, a comparison was made between the estimation accuracy of the proposed method and that of the previous method relying on the damper's mechanical model. The comparison results highlight the superiority of the proposed method.

The original contribution of this paper is to develop a novel tension estimation method for a cable with a damper free from the damper's complex stiffness by using the constraint equations that the measured and theoretical mode shapes are equal. The formulation will be explained in 2.4. Since the mode shapes are free from the damper's complex stiffness, the proposed method is free from the damper's modeling error. On the contrary, the previously proposed methods for a cable with a damper used the constraint equations based on the equality of the measured and theoretical natural frequencies (Furukawa *et al.*2021a, 2022d, 2022e), as will be explained in 2.3. The most recently proposed tension estimation method for a cable equipped with two dampers also used constraint equations based on the measured and theoretical natural frequencies (Furukawa *et al.*2023). Since the natural frequencies depend on the damper's complex stiffness, the previous methods cannot avoid the influence of the damper's modeling error. The proposed method solves this matter by using the constraint equations based on the mode shapes.

2. Previously proposed and newly proposed methods for estimating tension of cable with damper

2.1 Definition of coordinate axes and parameters

This paper proposes a tension estimation method for a cable with a damper for cable-stayed bridges. Fig. 1 shows the analytical model. The damper divides the cable into two sections. Each section ($d = 1,\ 2$) has a coordinate axis x_d, and the deflection at coordinate x_d at time t is defined as $y_d(x_d, t)$. The cable length is L, and the length of each section is l_d. It is assumed that the left end is the girder side, while the right end is the tower side, and the damper is attached near the girder. Therefore, the span length on the girder side l_1 is shorter than that on the tower side l_2. The cable is modeled as a tensioned Euler–Bernoulli beam, and both ends are assumed to have simple support. The tension T, bending stiffness EI, cross-sectional area A, and density ρ are assumed to be uniform throughout the cable. The damper is modeled as a complex spring, and its stiffness is k^*.

2.2 Vibrarion equation of tensioned Bernoulli–Euler beam

The deflection of the cable for each section follows the vibration equation for a tensioned

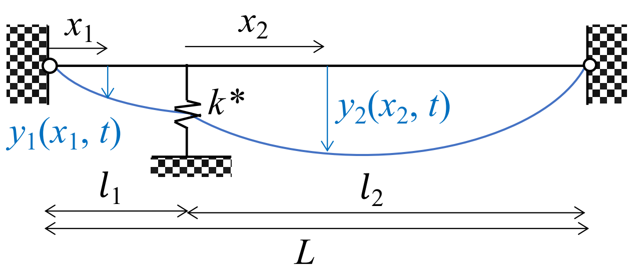

Fig. 1 Analytical model of cable with damper.

Euler–Bernoulli beam, as follows

$$\rho A\frac{\partial^2 y_d(x_d,t)}{\partial t^2} - T\frac{\partial^2 y_d(x_d,t)}{\partial {x_d}^2} + EI\frac{\partial^4 y_d(x_d,t)}{\partial {x_d}^4} = 0 \qquad (d = 1, 2) \tag{1}$$

Eq. (1) can be solved using the variable separation method; $y_d(x_d, t)$ is expressed as follows

$$y_d(x_d, t) = Y_d(x_d)\exp(2\pi jft) \tag{2}$$

where $Y_d(x_d)$ is the modal function, j is the imaginary unit, and f is the frequency. By substituting Eq. (2) into Eq. (1), a general solution for the modal function $Y_d(x_d)$ can be obtained as follows

$$Y_d(x_d) = C_{d1}\cos\alpha x_d + C_{d2}\sin\alpha x_d + C_{d3}\exp(\beta x_d) + C_{d4}\exp(-\beta x_d) \tag{3}$$

where C_{d1}, C_{d2}, C_{d3}, and C_{d4} are integral constants, and α and β are expressed by Eqs. (4) and (5), respectively.

$$\alpha = \sqrt{\sqrt{\left(\frac{T}{2EI}\right)^2 + \frac{\rho A(2\pi f)^2}{EI}} - \frac{T}{2EI}} \tag{4}$$

$$\beta = \sqrt{\sqrt{\left(\frac{T}{2EI}\right)^2 + \frac{\rho A(2\pi f)^2}{EI}} + \frac{T}{2EI}} \tag{5}$$

There are eight integral constants (C_{d1}, C_{d2}, C_{d3}, and C_{d4} for $d = 1, 2$); therefore, eight boundary conditions are required.

First, the following equations are obtained because both ends of the cable have simple supports

$$Y_1(0) = 0 \tag{6}$$

$$\frac{d^2 Y_1(0)}{d{x_1}^2} = 0 \tag{7}$$

$$Y_2(l_2) = 0 \tag{8}$$

$$\frac{d^2Y_2(l_2)}{dx_2{}^2} = 0 \tag{9}$$

Then, the following continuity equations are obtained at the damper position

$$Y_1(l_1) = Y_2(0) \tag{10}$$

$$\frac{dY_1(l_1)}{dx_1} = \frac{dY_2(0)}{dx_2} \tag{11}$$

$$\frac{d^2Y_1(l_1)}{dx_1^2} = \frac{d^2Y_2(0)}{dx_2^2} \tag{12}$$

Thus, seven equations were developed for eight integral constants.

2.3 Previously proposed tension estimation method depending on damper formula

As mentioned above, seven equations were developed for the eight integral constants, and one additional equation is required. In previous methods (Furukawa *et al.* 2021a, 2022d, 2022e), the equation of the equilibrium of forces at the damper position (Eq. (13)) was used for the 8$^{\text{th}}$ equation.

$$EI\frac{d^3Y_1(l_1)}{dx_1^3} - EI\frac{d^3Y_2(0)}{dx_2^3} = k^*Y_1(l_1) \tag{13}$$

where k^* is the damper's complex stiffness. Thus, eight equations were developed for eightintegral constants. By substituting Eq. (3) into Eqs. (6)-(13) and rearranging, a simultaneous linear equation for eight integral constants is obtained.

$$[\mathbf{D}]\{\mathbf{C}\} = \{\mathbf{0}\} \tag{14}$$

where $\{\mathbf{C}\} = \{C_{11} \cdots C_{14}\ C_{21}\ \cdots\ C_{24}\}^T$, and $[\mathbf{D}]$ is a coefficient matrix. For Eq. (14) to have a non-zero vector solution, the determinant of the coefficient matrix $[\mathbf{D}]$ must be zero.

$$\det[\mathbf{D}] = 0 \tag{15}$$

Eq. (15) can be rewritten as follows

$$\sin\alpha L\left\{\alpha^2 + \beta^2 + \frac{k^*}{EI}\left(\frac{\sin\alpha l_1 \cos\alpha l_1}{\alpha} - \frac{\sinh\beta l_1 \sinh\beta l_2}{\beta\sinh\beta L}\right)\right\} - \cos\alpha L\left(\frac{k^*}{EI}\frac{\sin^2\alpha l_1}{\alpha}\right) = 0 \tag{16}$$

As expressed by Eqs. (4) and (5), α and β depend on the frequency f. The frequency f at which Eq. (16) holds is the natural frequency, and there exists an infinite number of natural frequencies satisfying Eq. (16). By arranging the natural frequencies in ascending order, the i^{th} natural frequency is defined as f_i. In the following text, the variables corresponding to the i^{th} natural frequency f_i are denoted by subscript i.

Then, Eq. (16) can be written as follows

$$G_{1\mathrm{i}}\sin\alpha_i L - G_{2i}\cos\alpha_i L = 0 \tag{17}$$

where G_1 and G_2 are expressed as follows

$$G_{1i} = {\alpha_i}^2 + {\beta_i}^2 + \frac{k^*}{EI}\left(\frac{\sin\alpha_i l_1 \cos\alpha_i l_1}{\alpha_i} - \frac{\sinh\beta_i l_1 \sinh\beta_i l_2}{\beta_i \sinh\beta_i L}\right) \tag{18}$$

$$G_{2i} = \frac{k^*}{EI}\frac{\sin^2\alpha_i l_1}{\alpha_i} \tag{19}$$

The magnitudes of G_{i1} and G_{i2} in Eq. (17) differ depending on the mode, and normalization is carried out as follows

$$F_i \equiv \frac{G_{1i}}{\sqrt{G_{1i}^2 + G_{2i}^2}} \sin\alpha_i L + \frac{G_{2i}}{\sqrt{G_{1i}^2 + G_{2i}^2}} \cos\alpha_i L = 0 \tag{20}$$

Function F_i, which is defined in Eq. (20), is the tension estimation constraint equation that the natural frequency of a cable with a damper must satisfy. The i^{th} natural frequencies f_i are not explicitly included in Eq. (20), but are implicitly included through variables α_i and β_i

$$\alpha_i = \sqrt{\sqrt{\left(\frac{T}{2EI}\right)^2 + \frac{\rho A(2\pi f_i)^2}{EI}} - \frac{T}{2EI}} \tag{21}$$

$$\beta_i = \sqrt{\sqrt{\left(\frac{T}{2EI}\right)^2 + \frac{\rho A(2\pi f_i)^2}{EI}} + \frac{T}{2EI}} \tag{22}$$

The dampers are modeled using complex springs; therefore, the natural frequency f_i is also a complex value.

$$f_i = f_i^m(1 + jH_i) \tag{23}$$

where f_i^m is the real part of the complex natural frequency, and can be measured from the cable's free vibration response; H_i is the ratio of the imaginary part to the real part of the complex natural frequency, and is associated with a damping factor. Because the accurate measurement of the damping factor is difficult, this study considered H_i to be unknown.

The constraint function F_i defined in Eq. (20) is a complex function, and thus Eq. (20) holds for the real and imaginary parts, respectively. Therefore, the tension and other parameters can be estimated by solving the following optimization problem.

$$\min\sum_{i=1}^{n}\left\{\left(\mathrm{Re}\left(F_i(T, EI, k^*, H_i)\right)\right)^2 + \left(\mathrm{Im}\left(F_i(T, EI, k^*, H_i)\right)\right)^2\right\} \tag{24}$$

where n is the total number of natural frequencies used in the estimation. The real parts of the complex natural frequencies f_i^m $(i = 1, \dots, n)$ are obtained by measurement. The density ρ, cross-sectional area A, length L, and damper positions l_1 are assumed to be known from the design documents.

The proposed method estimates the unknowns by solving the nonlinear optimization problem in

Eq. (24). The unknown values are the cable tension T, bending stiffness EI, complex stiffness k^* of the damper, and ratio of the imaginary part of the complex natural frequency to the real part of the complex natural frequency H_i $(i = 1, \ldots, n)$. For the damper, the unknowns depend on the damper models. In the case of a high-damping rubber damper and a viscous shear damper, the design formula for the complex stiffness is expressed as follows

$$k_i^* = \begin{cases} k_u + jk_v & \text{(formula for high} - \text{damping rubber damper)} \qquad (25a) \\ k + j\big(2\pi f_i^m(1 + jH_i)\big)c & \text{(formula for viscous shear damper)} \qquad (25b) \end{cases}$$

In the high-damping rubber damper, k_u and k_v are the unknowns; in the viscous shear damper, k and c are the unknowns. Therefore, this study estimated both the real and imaginary part of the complex stiffness. Because a damper has two unknowns, the total number of unknowns is $4 + n$ variables (T, EI, k_u or k, k_v or c, H_i $(i = 1, \ldots, n)$). However, because the constraint equation in Eq. (20) holds for the real and imaginary parts, the number of constraint equations is $2n$. Therefore, to have more constraint equations than unknowns, the number of the real parts of the natural frequencies f_i^m required for estimation is at least 5 $(4 + n < 2n)$.

In the previously proposed method for tension estimation, the formula of the damper's complex stiffness must be determined in advance. The previous study assumed the use of a damper design formula. However, experimental verification revealed that the damper design formula, while intended for design purposes, does not consistently reflect the actual behavior, and the difference between the actual behavior and the damper formula becomes more pronounced at higher frequency. Therefore, the damper formula must be revised to better reproduce the actual damper behavior. In a previous paper, the authors proposed a refined damper formula for the high-damping rubber damper by introducing a frequency-dependent term in the imaginary part of the complex stiffness (Furukawa *et al.* 2023). The refined formula for a high-damping rubber damper is expressed as follows

$$k_s^* = k_u + j\{k_v + (2\pi f_i)^2 c\} \tag{26}$$

However, improving the damper formula for all types of dampers is labor intensive. Furthermore, the refined damper formula cannot solve the damper's amplitude dependence.

2.4 Newly proposed tension estimation method independent of damper formula

In the previous method, the force balance equation at the damper position expressed by Eq. (13) was used. As long as the force balance equation is used, a formula for the complex stiffness of the damper is required. Therefore, a new method that is independent of the damper formula is proposed. This study used mode shapes instead of the force balance equation.

By substituting Eq. (3) into Eqs. (6)-(12), seven simultaneous equations can be obtained for eight integral constants (C_{d1}, C_{d2}, C_{d3}, and C_{d4} for $d = 1,\ 2$). Therefore, seven integral constants can be expressed with one integral constant. This study used C_{12} to express the other seven integral constants; C_{21}, C_{22}, C_{23}, and C_{24} for the second span (d=2) are expressed with C_{12} as follows.

$$C_{21} = C_{12} \sin \alpha l_1 \tag{27}$$

$$C_{22} = -C_{12} \frac{\sin \alpha l_1}{\sin \alpha l_2} \cos \alpha l_2 \tag{28}$$

$$C_{23} = -C_{12} \frac{\alpha \sin \alpha L \sinh \beta l_1}{\beta \sin \alpha l_2 \sinh \beta L} \sinh \beta l_2 \tag{29}$$

$$C_{24} = C_{12} \frac{\alpha \sin \alpha L \sinh \beta l_1}{\beta \sin \alpha l_2 \sinh \beta L} \cosh \beta l_2 \tag{30}$$

Therefore, the theoretical mode shape for the second span (d=2) can be written as follows by substituting Eqs. (27)-(30) into Eq. (3) and dividing by C_{12}. The mode shape can be divided by C_{12} because the amplitude itself has no physical meaning. As mentioned previously, the variables corresponding to the i^{th} mode are denoted by subscript i. The theoretical mode shape of the i-th mode at x_2 is the function of tension T, bending stiffness EI, and ratio of the imaginary part to the real part of the complex natural frequencies H_i $(i = 1, \dots, n)$ since they are included in α_i and β_i of Eqs. (21) and (22).

$$\phi_i^t(x_2, T, EI, H_i) = \frac{\sin \alpha_i l_1}{\sin \alpha_i l_2} \sin \alpha_i (l_2 - x_2) - \frac{\alpha_i \sin \alpha_i L \sinh \beta_i l_1}{\beta_i \sin \alpha_i l_1 \sinh \beta_i L} \sinh \beta_i (l_2 - x_2) \tag{31}$$

Because the cable with a first span (d=1) is typically inside a steel pipe, it is practical to install accelerometers only on the second span (d=2). Therefore, it is assumed that accelerometers are placed on the second span of the cable to measure the mode shape. In the new method, the constraint equation is used, where the ratio of the theoretical two-point mode shapes equals the ratio of the measured two-point mode shapes. If the accelerometers are placed at $x_2 = p_1$ and $x_2 = p_I$, the constraint equation becomes as follows

$$\frac{\left|\phi_i^t(p_I, T, EI, H_i)\right|}{\left|\phi_i^t(p_1, T, EI, H_i)\right|} = \frac{\left|\phi_i^m(p_I)\right|}{\left|\phi_i^m(p_1)\right|} \quad (I = 2, 3, \dots) \tag{32}$$

where superscript t denotes the theoretical value and m denotes the measured value. The absolute values of the mode shapes are taken, and the mode shapes are normalized such that the larger value becomes equal to one. Next, to consider the case wherein the denominator of Eq. (32) is zero, the constraint equation is rewritten as follows

$$\left|\phi_i^t(p_1, T, EI, H_i)\right| \left|\phi_i^m(p_I)\right| - \left|\phi_i^t(p_I, T, EI, H_i)\right| \left|\phi_i^m(p_1)\right| = 0 \quad (I = 2, 3, \dots) \tag{33}$$

The proposed method seeks to determine the unknowns, tension T, bending stiffness EI, and ratio of the imaginary part to the real part of the complex natural frequencies H_i $(i = 1, \dots, n)$ by solving the following minimization problem, given the length L, l_1, l_2, density ρ, cross-sectional area A, the real parts of the eigenfrequencies of the first n modes $f_i{}^m$, and the mode shapes of the first n modes at N points $x_2 = p_1, \cdots, p_N$.

$$min \sum_{I=2}^{N} \sum_{i=1}^{n} \left\{ \left|\phi_i^t(p_1, T, EI, H_i)\right| \left|\phi_i^m(p_I)\right| - \left|\phi_i^t(p_I, T, EI, H_i)\right| \left|\phi_i^m(p_1)\right| \right\}^2 \tag{34}$$

where n is the total number of modes used in the estimation. The proposed method has $n(N-1)$ constraint equations for $2 + n$ unknowns. If the mode shapes are measured at three locations ($N = 3$), the natural frequencies and mode shapes of at least three modes are necessary to have more constraint equations than unknowns ($n(N-1) > 2 + n$).

Table 1 Cable parameters of numerical models

Cable No.	Length L [m]	Tension T [kN]	Mass per unit length ρA [kg/m]	Bending stiffness EI [kN $\cdot$ m^2]
10	25	1650	30.1	106.4
20	25	3300	30.1	106.4
30	50	3300	30.1	106.4
40	100	3300	30.1	106.4
50	200	1650	30.1	106.4
60	200	3300	30.1	106.4
70	200	5340	94.7	1111
80	200	10680	94.7	1111
90	500	9030	160.1	3175
100	500	18060	160.1	3175

To solve the nonlinear optimization problem, the MultiStart method is used to prevent locally optimal solutions. This method generates multiple initial values for the parameters to be estimated. Then, the optimal solution is sought using the nonlinear least-squares method for each initial value. The optimal solution minimizing Eqs. (24) and (28) is the global optimal solution. This study used 200 initial values for the MultiStart method.

3. Numerical verification

3.1 Numerical models and estimation condition

Numerical simulations were conducted to validate the proposed method. The tension T, bending stiffness EI, and ratio of the imaginary part to the real part of the complex natural frequencies H_i $(i = 1, \ldots, n)$ were estimated by inputting the real part of the theoretical complex natural frequencies and theoretical modes shapes into f_i^m and $\phi_i^m(p_I)$ $(i = 1, \ldots, n,\ I = 1,\ 2,\ 3)$ of the proposed optimization problem (Eq. (34)). The two types of dampers, high-damping rubber damper, and viscous shear damper expressed by Eqs. (25(a)) and (25(b)) were assumed.

By combining 10 cable models and nine damper models, a total of 90 models were used to verify the proposed method. Table 1 lists the cable specifications. Tables 2 and 3 list the damper specifications. The model number is the sum of the cable and damper model numbers. For example, model No. 11 consists of cable No. 10 and damper No. 1.

As presented in Table 1, the cable length increases with the cable number. The damper position, real part of the damper's complex stiffness for both damper types, and imaginary part of the damper's complex stiffness for the high-damping rubber dampers k_v are listed in Table 2. Regarding the viscous shear dampers, the imaginary part of the complex stiffness is defined by the damping coefficient c are listed in Table 3. The value of the damping coefficient c is calculated by $c = k_v/2\pi f_1^m$ such that the imaginary part of the damper's complex stiffness of the first-mode is equal between the two damper types.

It was assumed that the mode shapes are measured at three locations: 0.5 m, 1.0 m, and 1.5 m from the damper attachment point ($p_1 = 0.5,\ p_2 = 1.0,\ p_3 = 1.5$). The accelerometers were

Table 2 Damper parameters except for damping coefficient of viscous shear damper

Damper No.	Position l_1 [m]	Real part of damper's complex stiffness k_u or k [kN/m]	Imaginary part of damper's complex stiffness (for high-damping rubber damper) k_v [kN/m]
1	7	280.00	0.00
2	7	236.91	149.25
3	2	473.81	298.50
4	4.5	473.81	298.50
5	7	473.81	298.50
6	7	947.62	597.00
7	7	560.00	0.00
8	7	531.79	175.49
9	7	341.44	443.87

assumed to be placed near the girder, considering the efficiency of inspection work. The natural frequencies and mode shapes of the first to fifth modes or first to seventh modes were used. As mentioned earlier, with three mode shape measurement locations, at least three modes are needed to have more constraint equations than unknowns. Therefore, five or seven modes were used in the numerical simulation.

The parameters that were estimated are the cable tension (T), bending stiffness (EI), and ratio of the imaginary part to the real part of the complex natural frequencies of the 1st–5th or 1st–7th modes ($H_1, \ldots, H_5$ or $H_1, \ldots, H_7$). Therefore, seven or nine unknowns were estimated. In the search for solutions to the optimization problem, the tension and bending stiffness were set within the range of half to two times the true values, while the ratio of the imaginary part to the real part of the complex natural frequencies was set within the range of 0–1.

3.2 Estimation results

Figs. 2 and 3 show the estimation results for the tension and bending stiffness for two types of dampers when the first to fifth modes are used. Fig. 4 and 5 show the estimation results for two types of dampers when the first to seventh modes are used. The horizontal axis is the model number, and the vertical axis is the ratio of the estimated value to the true value. The estimation becomes more accurate as the vertical axis approaches 1.

This study confirmed that the proposed method can estimate the tension with high accuracy and a maximum estimation error of 0.68% for the high-damping rubber damper (Fig. 2(a)) and 0.70% for the viscous shear damper (Fig. 3(a)) when the first five modes are used, and 0.59% for the high-damping rubber damper (Fig. 4(a)) and 0.51% for the viscous shear damper (Fig. 5(a)) when the first seven modes are used. By comparing the estimation results in Figs. 2(a) and 4(a) and Figs. 3(a) and 5(a), it can be seen that the tension estimation accuracy is higher when the first seven modes are used compared with when the first five modes are used, because more data are used for tension estimation.

However, the bending stiffness estimation accuracy is lower compared with the tension estimation accuracy except for model Nos. 11–29 with a short cable length of 25 m when the first

Table 3 Damping coefficient of viscous shear damper

Model No.	Damping coefficient c $[\mathrm{kN \cdot s/m}]$	Model No.	Damping coefficient c $[\mathrm{kN \cdot s/m}]$	Model No.	Damping coefficient c $[\mathrm{kN \cdot s/m}]$
11	0.0	12	4.4	13	9.8
14	9.0	15	8.2	16	15.5
17	0.0	18	4.8	19	12.1
21	0.0	22	3.3	23	7.0
24	6.6	25	6.2	26	11.6
27	0.0	28	3.6	29	9.3
31	0.0	32	6.8	33	14.2
34	13.8	35	13.3	36	25.8
37	0.0	38	7.8	39	19.7
41	0.0	42	14.0	43	28.6
44	28.1	45	27.6	46	54.5
47	0.0	48	16.2	49	41.0
51	0.0	52	39.8	53	80.8
54	80.0	55	79.1	56	157.5
57	0.0	58	46.5	59	117.5
61	0.0	62	28.3	63	57.3
64	56.8	65	56.3	66	111.9
67	0.0	68	33.1	69	83.7
71	0.0	72	39.7	73	79.9
74	79.5	75	78.8	76	156.6
77	0.0	78	46.3	79	117.3
81	0.0	82	28.2	83	56.5
84	56.4	85	56.1	86	111.5
87	0.0	88	33.0	89	83.5
91	0.0	92	99.8	93	200.0
94	199.7	95	199.2	96	397.4
97	0.0	98	117.1	99	296.4
101	0.0	102	70.6	103	141.4
104	141.3	105	141.1	106	281.7
107	0.0	108	83.0	109	209.9

seven modes are used (Figs. 2(b), 3(b), 4(b), 5(b)). Because the mode shape measurement interval is fixed at 5 m, shorter cables have a relatively wider measurement range compared with longer cables, and higher modes have a shorter wave length, resulting in higher accuracy owing to the higher spatial resolutions. For a cable with dampers, the higher mode dissipates quickly and the higher-mode natural frequencies are difficult to estimate. A previous study (Furukawa *et al.* 2022d) measured the natural frequencies and mode shapes of a cable with a damper only up to the seventh modes. In practice, the accurate estimation of bending stiffness for a long cable is considered difficult.

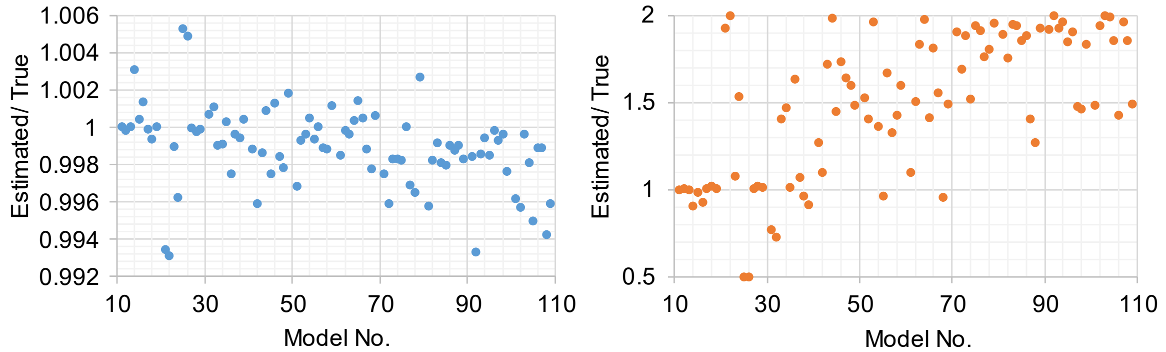

(a) Tension (b) Bending stiffness

Fig. 2 Ratio of estimated value to true value of tension and bending stiffness for high-damping rubber damper when 1st–5th modes are used

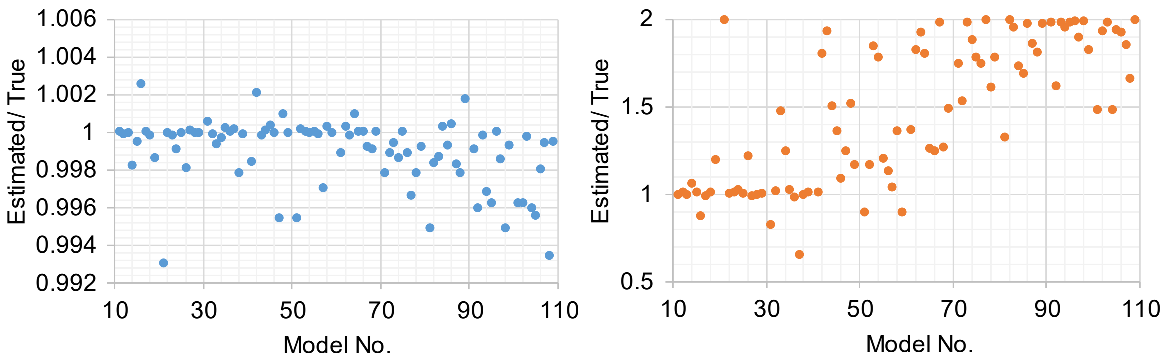

(a) Tension (b) Bending stiffness

Fig. 3 Ratio of estimated value to true value for tension and bending stiffness for viscous shear damper when 1st–5th modes are used

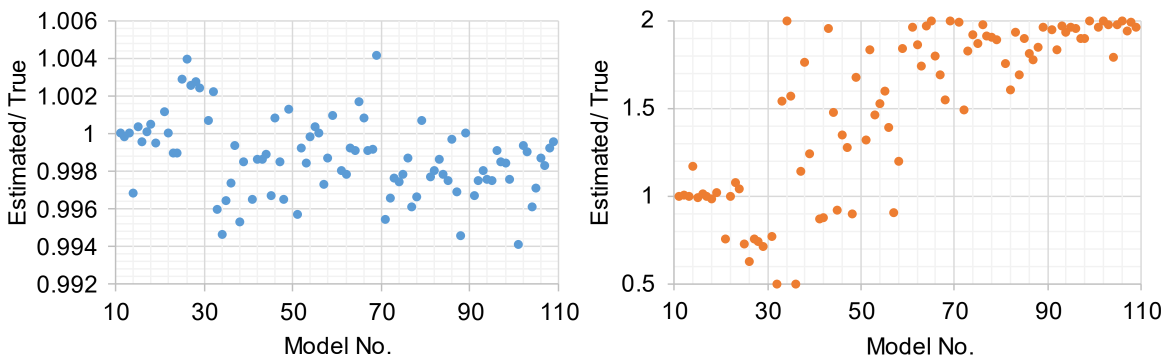

(a) Tension (b) Bending stiffness

Fig. 4 Ratio of estimated value to true value for tension and bending stiffness for high-damping rubber damper when 1st–7th modes are used

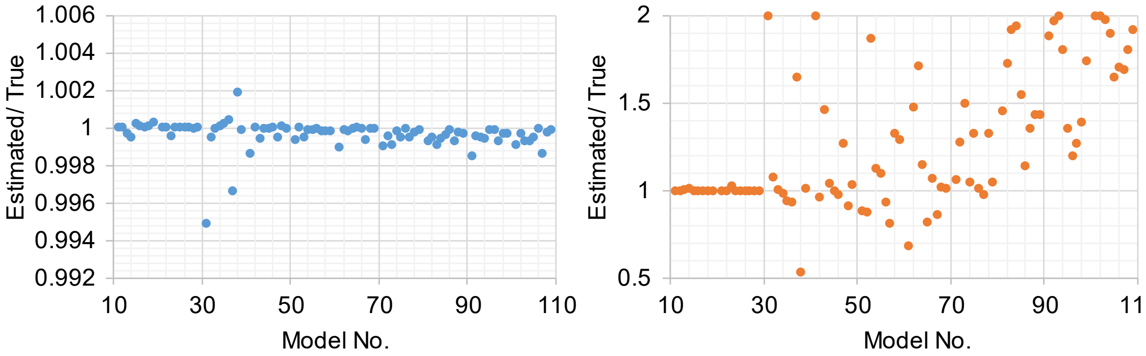

(a) Tension (b) Bending stiffness

Fig. 5 Ratio of estimated value to true value for tension and bending stiffness for viscous shear damper when 1st–7th modes are used

The estimation results for the ratio of the imaginary part to the real part of the complex natural frequencies are not shown, but the accuracy is low. This tendency is the same as that of the natural frequency-based tension estimation method for a cable with a damper (Furukawa *et al.* 2021a, 2022d, 2022e, 2022f, 2023).

The results reveal that the proposed method can estimate the cable tension with high accuracy, but the estimation accuracy of the other parameters is low. Therefore, the proposed method should only be used for cable tension estimation.

4. Experimental verification

4.1 Overview of experiment

The proposed method was experimentally validated using a horizontal cable. The experimental setting is shown in Fig. 6. A load cell was installed at the right end, and the tension value of the load cell was considered as the true tension value. The cable was hit with a hammer between the damper position and the right end. The acceleration histories were measured by piezoelectric accelerometers magnetically attached to the cable at three locations. The natural frequencies were measured by reading the peak frequencies of the acceleration Fourier spectra and used as the real part of the complex natural frequencies. The absolute values of the mode shapes were estimated from the acceleration Fourier amplitude at the natural frequencies.

The cable parameters are listed in Table 4. The prestressed steel strand with an outer diameter of 0.0286 m was used in this study. The test cases are listed in Table 5 with the cable's true tension and damper parameters. Three high-damping rubber dampers were used and the dampers' complex stiffness values listed in Table 5 were taken as the design values. The damper was placed at a distance l_1 from the left end. In cases No. 1–12, the tension is approximately 180 kN. In cases No. 13–24, the tension is approximately 380 kN.

Table 6 lists the first to seventh measured natural frequencies, arranged in ascending order. Table 7 lists the first to seventh measured mode shapes with the location of three measurement points (p_1, p_2, p_3).

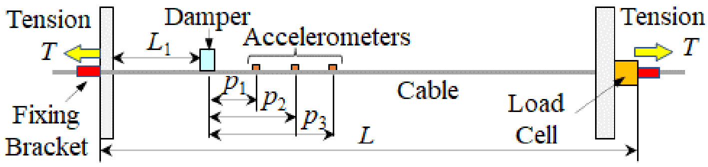

(a) Schematic diagram of test specimen, impact position, and measurement locations.

(a) Photo of test specimen

Fig. 6 Schematic diagram and photo of test specimen.

Table 4 Cable parameters of test specimen

Length (measured value) L [m]	Mass per unit length (catalog value) ρA [kg/m]	Bending stiffness (design value) EI [kN $\cdot$ m^2]
61.8	4.26	3.219

The mode shape measurement locations varied slightly depending on the test cases, but were generally 1 m, 1.5 m, and 2 m from the damper installation location. The natural frequencies and mode shapes of the first to seventh modes were input into the proposed method to estimate the tension. For comparison, only the natural frequencies of the first to seventh modes were input into the previously proposed method (Eq. (24)). By comparing the estimated tension with the load cell values, the accuracy of the proposed method and previously proposed method was confirmed. In the search for solutions to the optimization problem, the tension and bending stiffness values were set in the range of 0.3–10 times the true or design values, and the ratio of the imaginary part to the real part of the complex natural frequencies was set in the range of 0–1. In the previously proposed method, the damper parameters k_u and k_v were set in the range of 0–10 times the design values, and c was set in the range of 0–1 based on a previous study (Furukawa *et al.* 2023).

4.2 Tension estimation result

Fig. 7 shows the tension estimation result obtained by the proposed method independent of the damper's complex stiffness. Because the tension estimation error of the higher-order vibration method for a cable without a damper has been reported as 5% (Kobelco Wire Company, 2024), this study set the target tension estimation error within 5%. Case No. 16 has the maximum estimation error of 11.4%. However, except for case No. 1, the maximum estimation error is 4.17% in case No. 1, and is smaller than 5%.

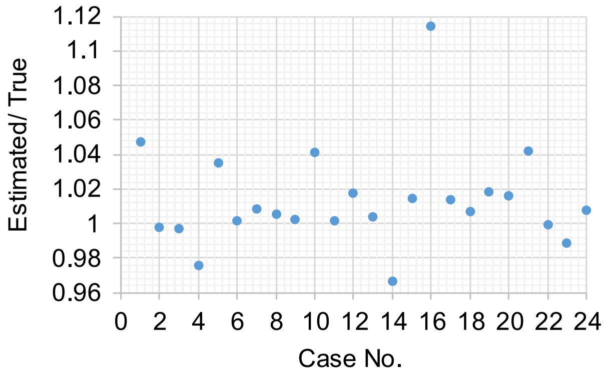

Fig. 7 Ratio of estimated tension to true tension by proposed method

Table 5 Test cases with cable's true tension and damper parameters (the dampers' complex stiffness is a designed value)

Case No.	Cable		Damper	
	True tension T [kN]	Position l_1[m]	Real part of damper's complex stiffness k_u[kg/m]	Imaginary part of damper's complex stiffness k_v [kg/m]
1	180.19	0.04	21.3	13.0
2	180.86	0.07	21.3	13.0
3	181.03	0.1	21.3	13.0
4	181.2	0.15	21.3	13.0
5	176.02	0.04	43.8	24.1
6	178.86	0.07	43.8	24.1
7	179.02	0.1	43.8	24.1
8	179.36	0.15	43.8	24.1
9	176.02	0.04	61.2	37.9
10	175.02	0.07	61.2	37.9
11	172.85	0.1	61.2	37.9
12	171.68	0.15	61.2	37.9
13	374.75	0.04	21.3	13.0
14	376.42	0.07	21.3	13.0
15	378.59	0.1	21.3	13.0
16	377.92	0.15	21.3	13.0
17	377.09	0.04	43.8	24.1
18	376.92	0.07	43.8	24.1
19	376.59	0.1	43.8	24.1
20	376.75	0.15	43.8	24.1
21	377.09	0.04	61.2	37.9
22	377.25	0.07	61.2	37.9
23	377.59	0.1	61.2	37.9
24	377.75	0.15	61.2	37.9

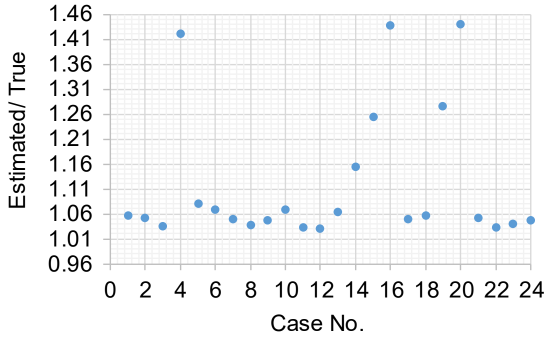

(a) Damper design formula

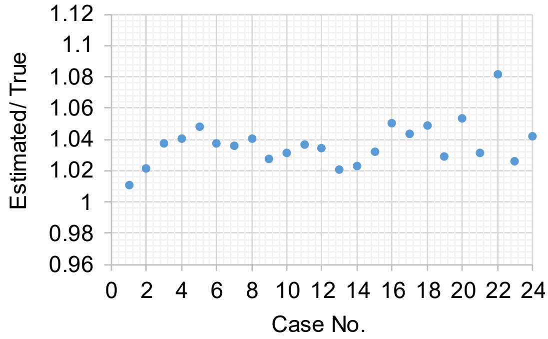

(b) Refined damper formula

Fig. 8 Ratio of estimated tension to true tension by previously proposed method using different damper formulas

Table 6 First to seventh measured natural frequencies in ascending order (Hz)

Case No.	1st	2nd	3rd	4th	5th	6th	7th
1	1.74	3.49	5.25	7.00	8.78	10.54	12.32
2	1.79	3.60	5.42	7.26	9.08	10.90	12.73
3	1.86	3.73	5.62	7.49	9.41	11.32	13.21
4	1.97	3.95	5.94	7.95	10.03	11.96	13.94
5	1.75	3.50	5.25	7.01	8.77	10.54	12.30
6	1.81	3.61	5.43	7.25	9.06	10.89	12.71
7	1.87	3.74	5.61	7.49	9.38	11.26	13.15
8	1.99	3.96	5.96	7.94	9.95	11.93	13.93
9	1.73	3.46	5.20	6.95	8.68	10.44	12.19
10	1.78	3.57	5.35	7.15	8.96	10.75	12.54
11	1.82	3.65	5.49	7.33	9.17	11.05	12.90
12	1.92	3.85	5.79	7.75	9.72	11.65	13.60
13	2.49	4.99	7.50	10.27	12.56	15.12	17.68
14	2.54	5.16	7.76	9.91	13.09	15.66	18.20
15	2.62	5.28	8.02	10.66	13.13	16.38	19.31
16	2.93	5.67	8.64	11.57	14.80	17.32	20.03
17	2.53	5.08	7.64	10.20	12.76	15.36	17.91
18	2.61	5.25	7.89	10.55	13.24	15.89	18.55
19	2.69	5.41	8.15	10.88	13.62	16.37	19.12
20	2.86	5.75	8.64	11.53	14.51	17.33	20.21
21	2.53	5.08	7.65	10.21	12.76	15.34	17.90
22	2.62	5.25	7.90	10.54	13.03	15.85	18.51
23	2.70	5.41	8.14	10.87	13.59	16.33	19.07
24	2.86	5.75	8.64	11.56	14.48	17.36	20.25

Table 7 First to seventh measured mode shapes in ascending order of corresponding natural frequencies

Case No.	p_1 [m] p_2 [m] p_3 [m]	Absolute value of mode shape						
		1st	2nd	3rd	4th	5th	6th	7th
1	1013.5	0.870	0.756	0.768	0.796	0.811	0.783	0.771
	1513.5	0.895	0.989	0.915	0.861	0.850	0.877	0.967
	2013.5	1.000	1.000	1.000	1.000	1.000	1.000	1.000
2	1013.5	0.793	0.843	0.958	0.914	0.798	0.834	0.848
	1513.5	0.837	0.923	0.932	0.915	0.889	0.884	0.887
	2013.5	1.000	1.000	1.000	1.000	1.000	1.000	1.000
3	1013.5	0.888	0.820	0.650	0.934	0.886	0.793	0.738
	1513.5	0.866	0.875	0.836	0.875	0.895	0.878	0.858
	2013.5	1.000	1.000	1.000	1.000	1.000	1.000	1.000
4	1013.5	0.844	0.835	0.865	0.841	0.751	0.785	0.810
	1513.5	0.934	0.872	0.789	0.850	0.843	0.781	0.844
	2013.5	1.000	1.000	1.000	1.000	1.000	1.000	1.000
5	1013.5	0.791	0.760	0.749	0.744	0.753	0.745	0.755
	1513.5	0.897	0.865	0.849	0.862	0.867	0.856	0.860
	2013.5	1.000	1.000	1.000	1.000	1.000	1.000	1.000
6	1013.5	0.797	0.774	0.763	0.786	0.785	0.758	0.772
	1513.5	0.862	0.859	0.852	0.875	0.868	0.864	0.870
	2013.5	1.000	1.000	1.000	1.000	1.000	1.000	1.000
7	1013.5	0.807	0.759	0.737	0.738	0.743	0.744	0.742
	1513.5	0.867	0.847	0.873	0.855	0.845	0.830	0.826
	2013.5	1.000	1.000	1.000	1.000	1.000	1.000	1.000
8	1013.5	0.796	0.952	0.795	0.962	0.788	0.793	0.800
	1513.5	0.854	0.995	0.881	1.000	0.869	0.883	0.889
	2013.5	1.000	1.000	1.000	0.998	1.000	1.000	1.000
9	1013.5	0.811	0.724	0.685	0.801	0.774	0.764	0.750
	1513.5	0.891	0.845	0.818	0.872	0.838	0.861	0.860
	2013.5	1.000	1.000	1.000	1.000	1.000	1.000	1.000
10	1013.5	0.901	0.681	0.694	0.802	0.895	0.800	0.731
	1513.5	0.980	0.900	0.886	0.879	0.864	0.880	0.889
	2013.5	1.000	1.000	1.000	1.000	1.000	1.000	1.000
11	1013.5	0.948	0.734	0.717	0.813	0.914	0.815	0.770
	1513.5	0.995	0.815	0.806	0.900	1.000	0.912	0.867
	2013.5	1.000	1.000	1.000	1.000	0.977	1.000	1.000
12	1013.5	0.740	1.000	1.000	0.768	0.709	0.730	0.810
	1513.5	0.951	0.937	0.796	0.855	0.848	0.860	0.883
	2013.5	1.000	0.992	0.756	1.000	1.000	1.000	1.000
13	1013.5	1.000	0.917	0.765	0.799	0.810	0.766	0.817
	1513.5	0.970	0.930	0.845	0.000	0.855	0.842	0.864
	2013.5	0.984	1.000	1.000	1.000	1.000	1.000	1.000
14	1013.5	1.000	0.919	1.000	1.000	1.000	1.000	1.000
	1513.5	1.000	0.890	0.960	0.923	0.966	0.975	0.966
	2013.5	1.000	1.000	0.954	0.820	0.998	0.972	0.935
15	1013.5	0.909	0.892	0.876	0.874	0.880	0.897	0.851
	1513.5	0.916	0.915	0.930	0.914	0.926	0.943	0.907
	2013.5	1.000	1.000	1.000	1.000	1.000	1.000	1.000

Table 7 Continued

16	513.5	0.970	0.986	0.991	0.997	1.000	0.775	0.939
	1013.5	1.000	1.000	1.000	1.000	0.994	0.919	1.000
	1513.5	0.865	0.909	0.899	0.908	0.956	1.000	0.932
17	1013.5	0.852	0.785	0.760	0.770	0.817	0.754	0.793
	1513.5	0.887	0.878	0.866	0.866	0.872	0.855	0.874
	2013.5	1.000	1.000	1.000	1.000	1.000	1.000	1.000
18	1013.5	0.828	0.780	0.764	0.759	0.751	0.741	0.762
	1513.5	0.907	0.848	0.847	0.844	0.839	0.836	0.851
	2013.5	1.000	1.000	1.000	1.000	1.000	1.000	1.000
19	1013.5	0.821	0.831	0.816	0.798	0.780	0.775	0.777
	1513.5	0.000	0.888	0.886	0.879	0.872	0.872	0.871
	2013.5	1.000	1.000	1.000	1.000	1.000	1.000	1.000
20	1013.5	0.897	0.774	0.789	0.764	0.740	0.764	0.772
	1513.5	0.935	0.867	0.864	0.849	0.846	0.861	0.865
	2013.5	1.000	1.000	1.000	1.000	1.000	1.000	1.000
21	1013.5	0.796	0.788	0.786	0.770	0.773	0.786	0.789
	1513.5	0.851	0.912	0.884	0.887	0.914	0.901	0.879
	2013.5	1.000	1.000	1.000	1.000	1.000	1.000	1.000
22	1013.5	0.641	0.747	0.853	0.967	1.000	0.856	0.827
	1513.5	0.769	0.824	0.890	0.947	0.743	0.896	0.895
	2013.5	1.000	1.000	1.000	1.000	0.786	1.000	1.000
23	1013.5	0.720	0.822	0.820	0.886	0.773	0.812	0.850
	1513.5	0.814	0.876	0.877	0.883	0.844	0.871	0.890
	2013.5	1.000	1.000	1.000	1.000	1.000	1.000	1.000
24	1013.5	0.747	0.790	0.778	0.791	0.802	0.773	0.923
	1513.5	0.846	0.859	0.862	0.869	0.880	0.867	0.976
	2013.5	1.000	1.000	1.000	1.000	1.000	1.000	1.000

Fig. 8(a) shows the tension estimation result obtained by the previously proposed method using the damper design formula for the high-damping rubber damper expressed by Eq. (25(a)). The estimation errors exceeded 40% in case Nos. 4, 16, and 20 when the damper design formula was used. The large estimation error was caused by the difference between the actual damper's complex stiffness and the design formula.

Next, Fig. 8(b) shows the tension estimation results obtained by the previously proposed method using the refined damper formula expressed by Eq. (26). This refined damper formula was developed such that that the theoretical natural frequencies match the observed natural frequencies (Furukawa *et al.* 2023). The maximum error occurred in case No. 22 and is 8.14%. The estimation errors exceeded 5% in case Nos. 16, 20, and 22.

With the proposed method, only case No. 16 exceeded the target estimation error of 5%. With the previously proposed method, the target estimation error of 5% was also exceeded in case No. 16. Therefore, it is possible that the larger measurement error is included in the natural frequencies and mode shapes for case No. 16.

4.3 Discussion

Table 8 compares the tension estimation accuracy using three error indices: the Root Mean Square Error Ratio (RMSER), Mean Absolute Error Ratio (MAER), and Maximum Error Ratio (MER) among the case wherein the proposed method was used, case wherein the previous method

Table 8 Tension estimation error by proposed method and previously proposed method with different damper formulas

	Proposed method	Previously proposed method using damper design formula	Previously proposed method using refined damper formula
RMSER	0.59%	3.38%	0.74%
MAER	1.97%	12.0%	3.67%
MER	11.4%	43.9%	8.14%
Second MER	4.17%	43.8%	5.31%

with the damper design formula was used, and case wherein the previous method with the refined damper formula was used. The three error indices were calculated using the following equations.

$$\mathrm{RMSER} = \sqrt{\frac{1}{24}\sum_{I=1}^{24}\left(\frac{T_I^{estimated}}{T_I^{true}} - 1\right)^2} \tag{35}$$

$$\mathrm{MAER} = \frac{1}{24}\sum_{I=1}^{24}\left|\frac{T_I^{estimated}}{T_I^{true}} - 1\right| \tag{36}$$

$$\mathrm{MER} = \max\left|\frac{T_I^{estimated}}{T_I^{true}} - 1\right| \tag{37}$$

is the true tension value of model number I.

The proposed method has the smallest RMSER and MAER among the three cases. The MER of the proposed method is not the smallest. However, the second MER of the proposed method is the smallest.

The estimation error indices of the previously proposed method are larger than those of the proposed method except No. 16, even when using the refined damper formula, which cannot model the actual damper behavior perfectly. The damper has frequency-dependence and amplitude-dependence. By introducing the imaginary stiffness term depending on the frequency, the refined damper model improved in terms of frequency dependence, but still does not consider the amplitude dependence. The proposed method is independent from the damper formula; therefore, it is free of the damper’s frequency and amplitude dependence and achieves higher tension estimation accuracy.

The proposed method is effective not only in terms of estimation accuracy, but also in terms of practicality, because it does not require the development of a refined model of the damper’s complex stiffness for each damper.

5. Conclusions

This study developed a tension estimation method for a cable with a damper that does not rely on the modeling error of the damper’s complex stiffness. The proposed method was numerically and experimentally validated and the following conclusions were drawn.

In previous tension estimation methods relying on the natural frequencies, the force balance equation must be incorporated at the damper installation point. This requirement entails employing the mechanical model of the damper's complex stiffness. However, because the actual damper behaves differently to the design formula, the tension estimation accuracy deteriorates owing to the damper modeling error. In the proposed method, by introducing new constraint equations related to the mode shapes, the force balance equation becomes unnecessary, and thus the tension is estimated independent of the mechanical model of the damper's complex stiffness.

In the numerical verification using 90 models, the proposed method estimated the tension accurately with an estimation error within 0.59%. However, the estimation accuracy of the bending stiffness was low, indicating that the proposed method is only practical for tension estimation.

In the experimental verification using 24 cases, the proposed method estimated the tension accurately with the estimation error within 11.4% for all cases and within 4.17% except for one case. On the other hand, the maximum estimation error of the previous method with a damper design formula was approximately 44%. The proposed method achieved better accuracy compared with the previous method, even with the refined damper formula, in terms of RMSER, MAER and the second MER.

This study developed an accurate tension estimation method for a cable with a damper based on the mode shapes. The proposed method eliminates damper modeling error, can estimate the tension without removing the dampers, and contributes toward reducing the effort and time of inspections, even when the damper behavior is unknown. The proposed method is effective not only in terms of estimation accuracy, but also in terms of practicality, because it does not require the development of a refined model of the damper's complex stiffness for each damper.

Acknowledgments

We thank Edanz (https://jp.edanz.com/ac) for editing a draft of this manuscript.

References

Chen, C.C., Wu, W.H., Leu, M.R. and Lai, G. (2016), "Tension determination of stay cable or external tendon with complicated constraints using multiple vibration measurements", *Measurement*, **86**, 182-195. https://doi.org/10.1016/j.measurement.2016.02.053.

Chen, C.C., Wu, W.H., Leu, M.R. and Lai, G. (2018), "A novel tension estimation approach for elastic cables by elimination of complex boundary condition effects employing mode shape functions", *Eng. Struct.*, **166**, 152-166. https://doi.org/10.1016/j.engstruct.2018.03.070.

Foti, F., Geuzaine, M. and Denoel, V. (2020), "On the identification of the axial force and bending stiffness of stay cables anchored to flexible supports", *Appl. Math. Model.*, **92**, 798-828. https://doi.org/10.1016/j.apm.2020.11.043.

Furukawa, A., Goda, K. and Takeichi, T. (2023), "Tension estimation method using natural frequencies for cable equipped with two dampers", *Struct. Monit. Maint.*, **10**(4), 361-379. https://doi.org/10.12989/smm.2023.10.4.361.

Furukawa, A., Hirose, K. and Kobayashi, R. (2021a), "Tension estimation method for cable with damper using natural frequencies", *Front. Built Environ.*, **7**(603857), https://doi.org/10.3389/fbuil.2021.603857.

Furukawa, A., Hirose, K. and Kobayashi, R. (2022d), “Tension estimation method for cable with damper and its application to real cable-stayed bridge”, (Eds., Wu, Z., Nagayama, T., Dang, J. and Astroza, R.), *Experimental Vibration Analysis for Civil Engineering Structures. Lecture Notes in Civil Engineering*, **224**. Springer, Cham. https://doi-org.kyoto-u.idm.oclc.org/10.1007/978-3-030-93236-7_32.

Furukawa, A., Kozuru, K. and Kobayashi, R. (2022c), “Method for estimating tension of two Nielsen–Lohse bridge cables with intersection clamp connection and unknown boundary conditions”, *Front. Built Environ.*, **8**(906871). https://doi.org/10.3389/fbuil.2022.993958.

Furukawa, A., Suzuki, S. and Kobayashi, R. (2022e), “Tension estimation method for cable with damper using natural frequencies with uncertain modal order”, *Front. Built Environ.*, **8**(812999). https://doi.org/10.3389/fbuil.2022.812999.

Furukawa, A., Suzuki, S. and Kobayashi, R. (2022f), “Tension estimation method for cable with damper using natural frequencies and two-point mode shapes with uncertain modal order”, *Front. Built Environ.*, **8**(906871). https://doi.org/10.3389/fbuil.2022.906871.

Furukawa, A., Yamada, S. and Kobayashi, R. (2022a), “Tension estimation methods for two cables connected by an intersection clamp using natural frequencies”, *J. Civ. Struct. Health Monit.*. **12**, 339-360. https://doi.org/10.1007/s13349-022-00548-6.

Furukawa, A., Yamada, S. and Kobayashi, R. (2022b), “Tension estimation methods for Nielsen-Lohse bridges using out-of-plane and in-plane natural frequencies”, *Int. J. Geomate*, **23**(97), 1-11. https://doi.org/10.21660/2022.97.3235.

Hou, J., Li, C., Jankowski, L., Shi, Y., Su, L., Yu, S. and Geng, T. (2020), “Damage identification of suspender cables by adding virtual supports with the substructure isolation method”, *Struct. Control Health Monit.*, **28**(3), e2677, https://doi.org/10.1002/stc.2677.

Izzi, M., Caracogilia, L. and Noe, S. (2016), “Investigating the use of Targeted-Energy-Transfer devices for stay-cable vibration mitigation”, *Struct. Control Health Monit.*, **23**, 315-332. https://doi.org/10.1002/stc.1772.

Javanbakht, M., Cheng, S. and Ghrib, F. (2019), “Control-oriented model for the dynamic response of a damped cable”, *J. Sound Vib.*, **442**, 249-267. https://doi.org/10.1016/j.jsv.2018.10.036.

Jeong, S., Kim H., Lee, J. and Sim, S.H. (2020), “Automated wireless monitoring system for cable tension force using deep learning”, *Struct. Health Monit.*, **20**(4), 1805-1821. https://doi.org/10.1177/1475921720935837.

Kim, B.H. and Park, T. (2007), “Estimation of cable tension force using the frequency-based system identification method”, *J. Sound Vib.*, **304**, 660-676. https://doi.org/10.1016/j.jsv.2007.03.012.

Kobelco Wire Company, Ltd. (2024), Tension measuring technique for outer cables. http://www.shinko-wire.co.jp/products/vibration.html [Accessed: January 30, 2024]. (In Japanese)

Krenk, S. (2000), “Vibration of a taut cable with an external damper”, *ASME, J. Appl. Mech.*, **67**, 772-776. https://doi.org/10.1115/1.1322037.

Lazar, I.F., Neild, S.A. and Wagg, D.J. (2016), “Vibration suppression of cables using tuned inerter dampers”, *Eng. Struct.*, **122**, 62-71. https://doi.org/10.1016/j.engstruct.2016.04.017.

Li, S., Wang, L., Wang, H., Shi, P., Lan, R., Wu, C. and Wang, X. (2021), “An accurate measurement method for tension force of short cable by additional mass block”, *Adv. Mater. Sci. Eng.*, **2021**(6622628), https://doi.org/10.1155/2021/6622628.

Liu G., Wang, X., Wang, X., Wan, Y. and Li, B. (2023), “Noncontact cable tension estimation using edge recognition technology based on convolutional network”, *Structures*, **58**(105337). https://doi-org.kyoto-u.idm.oclc.org/10.1016/j.istruc.2023.105337.

Ma, L. (2017), “A highly precise frequency-based method for estimating the tension of an inclined cable with unknown boundary conditions”, *J. Sound Vib.*, **409**, 65-80. https://doi.org/10.1016/j.jsv.2017.07.043.

Ma, L., Xu, H., Munkhbaatar, T. and Li, S. (2021), “An accurate frequency-based method for identifying cable tension while considering environmental temperature variation”, *J. Sound Vib.*, **490**(115693). https://doi.org/10.1016/j.jsv.2020.115693.

MathWorks. (2024), MATLAB Documentation, MultiStart, https://jp.mathworks.com/help/gads/multistart.html [Accessed: January 30, 2024].

Pacheco, B.M., Fujino, Y. and Sulekh, A. (1993), “Estimation curve for modal damping in stay cables with viscous damper”, *J. Struct. Eng.*, **119**(6), 1961-1979. https://doi.org/10.1061/(ASCE)0733-9445(1993)119:6(1961)

Shan, D., Zhou, X. and Khan, I. (2019), “Tension identification of suspenders with supplemental dampers for through and half-through arch bridges under construction”, *J. Struct. Eng. - ASCE*, **145**(3), Paper ID 04018265, https://doi.org/10.1061/(ASCE)ST.1943-541X.0002255.

Shi, X. and Zhu, S. (2018), “Dynamic characteristics of stay cables with inerter dampers”, *J. Sound Vib.* **423**, 287-305. https://doi.org/10.1016/j.jsv.2018.02.042.

Shinke, T., Hironaka, K., Zui, H. and Nishimura, H. (1980), “Practical formulas for estimation of cable tension by vibration method”, *J. Japan Soc. Civil Engineers*, **294**, 25-32. (In Japanese) https://doi.org/10.2208/jscej1969.1980.294_25.

Tabatabai, H. and Mehrabi, B. (2000), “Design of mechanical viscous dampers for stay cables”, *J. Bridge Eng.- ASCE*, **5**(2), 114-123. https://doi.org/10.1061/(ASCE)1084-0702(2000)5:2(114).

Weber, F. and Distl, H. (2015), “Amplitude and frequency independent cable damping of Sutong Bridge and Russky Bridge by magnetorheological dampers”, *Struct. Control Health Monit.*, **22**(2), 237-254. https://doi.org/10.1002/stc.1671.

Yamagiwa, I., Utsuno, H., Endo, K. and Sugii, K. (2000), “Identification of flexural rigidity and tension of one-dimensional structure by measuring eigenvalues in higher order”, *Transactions of the Japan Soc. Mech. Engineers*, **66**(649), 2905-2911. (In Japanese) https://doi.org/10.1299/kikaic.66.2905.

Yan, B., Chen, W., Dong, Y. and Jiang, X. (2020), “Tension force estimation of cables with two intermediate supports”, *Int. J. Struct. Stab. Dynam.*, **20**(3), Paper ID 2050032, https://dx.doi.org/10.1142/S0219455420500327

Yan, B., Chen., W., Yu, J. and Jiang, X. (2019), “Mode shape-aided tension force estimation of cable with arbitrary boundary conditions”, *J. Sound Vib.*, **440**, 315-331. https://doi.org/10.1016/j.jsv.2018.10.018.

Zarbaf, S.E.H.A.M., Norouzi, M., Allemang, R., Hunt, V. and Helmicki, A. (2017), “Stay cable tension estimation of cable-stayed bridges using genetic algorithm and particle swarm optimization”, *J. Bridge Eng.*, **22**(10), Paper ID 05017008. https://doi.org/10.1061/(ASCE)BE.1943-5592.0001130.

Zarbaf, S.E.H.A.M., Norouzi, M., Allemang, R., Hunt, V., Helmicki, A. and Venkatesh, C. (2018), “Vibration-based cable condition assessment: A novel application of neural networks”, *Eng. Struct.*, **177**, 291-305. https://doi.org/10.1016/j.engstruct.2018.09.060.

Zui, H., Sinke, T. and Namita, Y. (1996), “Practical formulas for estimation of cable tension by vibration method”, *J. Struct. Eng. - ASCE*, **122**(6), 651-656. https://doi.org/10.1061/(ASCE)0733-9445(1996)122:6(651).

JK